Morphological analysis of the diesel jet at the nozzle outlet

Yon J., Blaisot J.-B.

CORIA UMR 6614 : CNRS, Université et INSA de Rouen
Site universitaire du Madrillet, avenue de l'université
BP 12 76801 Saint Etienne du Rouvray, France
Phone : 33.(0)2.32.95.37.11 / fax : 33.(0)2.32.91.04.85
jerome.yon@coria.fr jean-bernard.blaisot@coria.fr

This article deals with the morphological shape of the Diesel jet in the vicinity of the nozzle outlet. Gray level pictures of the jet are taken for different injection pressures going from 15 to 100 MPa at different times from the start of the needle lift. The jet appears as black over white on the pictures. Binary images of the jet are decomposed in vertical and horizontal lines. Line length distributions are then calculated, allowing the determination of several morphological parameters. These parameters are linked to the dense jet diameter, the disturbance amplification, and the length, the thickness and the density of the ligaments. The variation of these quantitative parameters along the jet axis, gives information on the atomization of the jet.

1. Introduction

The decreasing of the pollutant emission of Diesel cars is a goal that stimulates industrialists and researchers to study the atomization processes in Diesel jet applications. Numerous studies have been published on this subject, particularly in the direct injection (DI) field. In the firsts steps of atomization several phenomena are taking place at the nozzle exit: the aerodynamic stripping of the jet, the transient behavior of the flow, the internal turbulence increased by the collapse of gas cavities... Numerous investigations techniques have been used in order to bring out information from this difficult-to-analyze jet: X-ray analysis[1], measurement of conductivity, laser sheet tomographic experiments, which showed the presence of cavitation in transparent nozzles[1] and directly in the jet[3][4]. All these experimental approaches gave qualitative information. The only quantitative measurements made concerning the Diesel jet are the length of liquid penetration and the cone angle.
In this paper, we present a statistical analysis based on shadowgraphy images through a morphological approach. Morphological parameters are extracted from the picture series for injection pressures going from 15MPa to 100 MPa and at different delay times during the injection.

2. Experimental setup

The analysis presented in this article is applied to Diesel jet pictures in the vicinity of a single orifice injector (*Ganser*). The nozzle orifice is 200 μm in diameter and 800 μm in length. The needle lift driving signal duration is about 2ms. The fuel is injected in quiescent air at normal pressure and temperature conditions. The axis of the injector is vertical. Images are obtained with a CCD camera (Sony XC8500CE, 763x581 pixels) linked to a long working distance microscope. In order to observe as long a part of the jet as possible, the camera is rotated 90

degrees. Thus, the field of view is 1.20 mm along the jet axis and and 1.08 mm in the radial direction. A white incoherent flash lamp (HSPS Nanolite) is used in a backlight configuration. The flash lasts 10 ns and enables the liquid structures on the jet to be frozen. In this optical configuration, the depth of field is very thin. The morphological analysis was conducted in two different ways. The first approach considers the temporal morphological evolution of the jet interface for two injection pressures: 20 MPa and 60 MPa. The fluctuation of the driving signal and the real start of the injection is avoided using a reference signal given by an infrared-led transceiver placed at the nozzle exit. A time-delay is then applied between this signal and the flash (red vertical lines on Fig. 2). The illumination time corresponds to a certain delay from the reference signal, which also corresponds to a certain position of the needle lift, independently measured (black curve in Fig. 2).

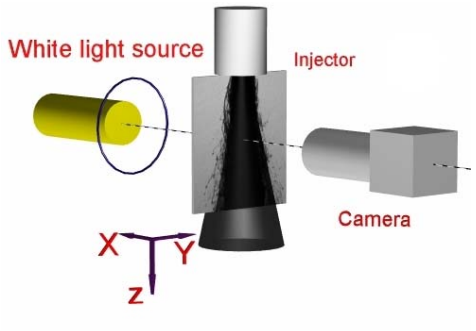

Fig. 1 Experimental set-up

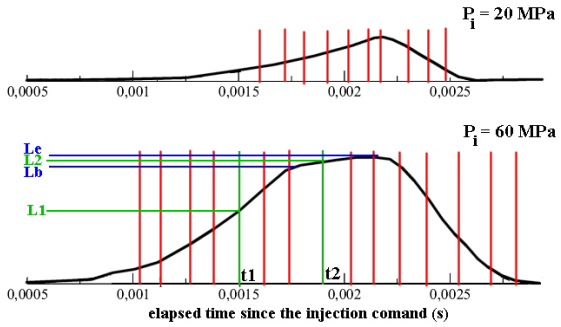

Fig. 2 Needle lift curves and illumination times

The second approach considers the effect of the pressure increase on the morphological aspect of the jet interface. The injection pressures vary from Pi=15MPa to 65MPa every 5MPa (Pi=80MPa and Pi=100MPa on certain cases). For each Pi, two illumination times are defined thanks to the needle lift curve. They are characterized thanks to the needle lift levels Lb and Le, represented in blue in Fig. 2. These levels determine the period of the quasi-static flow. The first delay time (t1) corresponds to the beginning of the injection, with an accelerating flow in the nozzle. This delay time corresponds to the level L1 equal to 79% of the level lift Lb. The second delay time t2, corresponds to the quasi-static flow defined by the lift L2 such as L2-Lb=52%(Le-Lb). For each pressure and delay time couple, a series of 400 pictures is considered.

3. Pre-processing of the picture series

The first operation consists in the normalization of the original grey level picture. This consists in dividing each picture by the background picture without jet. This gives a uniform grey level in the region of the gas phase. The morphological analysis is applied on two-level pictures. A specific thresholding technique that uses the wavelet transform has been used

(a): Original picture (b): After threshold (c): Isolation of the plain jet.

Fig. 3 The different steps of the image processing

here. This technique was developed for an image based granulometer [5]. One example of a 2 gray level picture is presented in Fig. 3(b).
The analysis presented here is focused on the morphology of the plain jet interface. The liquid phase that is already atomized is not taken into account. The picture shown in Fig. 3(c) is an example of a picture resulting from the separation of the jet and its surrounding spray. We can observe on this picture the presence of ligaments which are detaching from the Diesel plain jet. On this picture, we have also defined a region of interest (ROI), delimited by the grey box. The morphological analysis is done inside this ROI. The width and the distance of this ROI from the nozzle are varied.

4. The statistical morphological analysis

The morphological analysis is based on the successive applications of morphological operators such as opening and closing over the entire two level pictures. The surface change occurring after each operator application corresponds to a particular morphological behavior of the studied domain. In our case, the structural elements are simply vertical and horizontal lines. Thus, the analysis consists in calculating the length distribution of lines of pixels included in the ROI over the entire picture series. Then, we obtain distributions corresponding to black and white, vertical and horizontal lines that constitute the entire pictures.

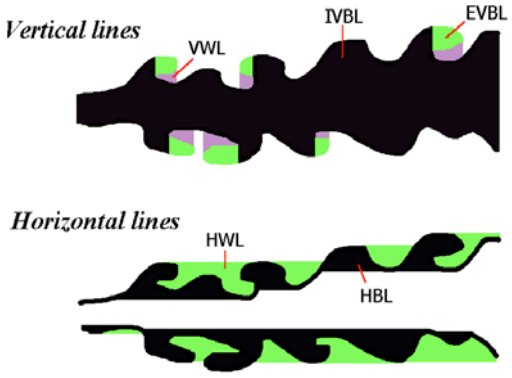

Three surfaces are computed from the vertical lines:

- IVBL : the vertical black lines which cross the jet axis.
- VWL : the vertical white lines confined between black vertical lines.
- EVBL : vertical black lines which do not cross the jet axis.

Two surfaces are computed from the horizontal lines :

- HWL : horizontal white lines embedded between two horizontal black ones.
- HBL : horizontal black lines which do not intercept the picture sides.

Fig. 4 Surface characterization

The different kinds of lines used to define different surfaces are distinguished in Fig. 4. Vertical lines are decomposed into three families giving rise to three kinds of surfaces: the black vertical lines which intercept the jet axis (IVBL), the black vertical lines which do not intercept the jet axis (EVBL) and the white vertical lines that are confined between black vertical lines (VWL).
The horizontal lines that do not intercept the picture edges are decomposed into two families. The white lines bounded by black lines form the surface area HWL and the black lines confined between white lines form the surface HBL. One example of application of the morphological analysis is presented in [4].
In order to define a dense core diameter ***D***, we must distinguish the surface corresponding to the dense part of the jet and the disintegrating part of it. The whole surface of the jet is equal to the sum of the surfaces IVBL and EVBL. The corrugated part of the jet or the ligament surface can be evaluated by the mean surface of HBL and EVBL. Thus, the surface corresponding to the dense part of the jet over the picture series is the entire jet surface minus the corrugated mean surface. The diameter is defined as this global surface divided by the width of the ROI ***l*** and the number of pictures ***nbi*** used in the line distribution computation.

$$D = \frac{IVBL + \frac{1}{2}(EVBL - HBL)}{l \cdot nbi} \qquad C_{av} = \frac{HWL - VWL}{IVBL + EVBL} \qquad t_l = \frac{EVBL}{nbl(EVBL)} \qquad l_l = \frac{nbl(EVBL)}{l \cdot nbi} \qquad d_l = \frac{EVBL}{VWL}$$

The ***concavity*** number, C_{av} is the area formed by the air horizontally embedded by the jet divided by the surface area of the jet. This parameter is relative to the macroscopic interface disturbances of the jet.
The t_l number is the mean thickness of the ligaments or protuberances that emanate from the jet where ***nbl(EVBL)*** is the number of lines that make up the ***EVBL*** surface.
l_l, corresponds to the mean total length of the ligaments found in the ROI, divided by ***l***. If this parameter is equal to 2, for example, this indicates that typically there are two ligaments along the jet (one per side for example). And, d_l is defined as the ligament surface area divided by the surface area of the air embedded by these ligaments. This gives us information on the density of the ligaments or protuberances formed by the jet.

5. Results

The results presented here correspond to a ROI width of 60 pixels (94 µm). The ROI is shifted along the jet axis by steps of 94 µm. Results for each parameter are presented hereafter. Figures presenting the variation of the parameters are separated in two parts: (a) the left part corresponds to the time evolution for two injection pressures 20 MPa and 60 MPa, (b) the right part corresponds to the effect of the pressure for the delay times t1 and t2.

5.1. The dense core diameter

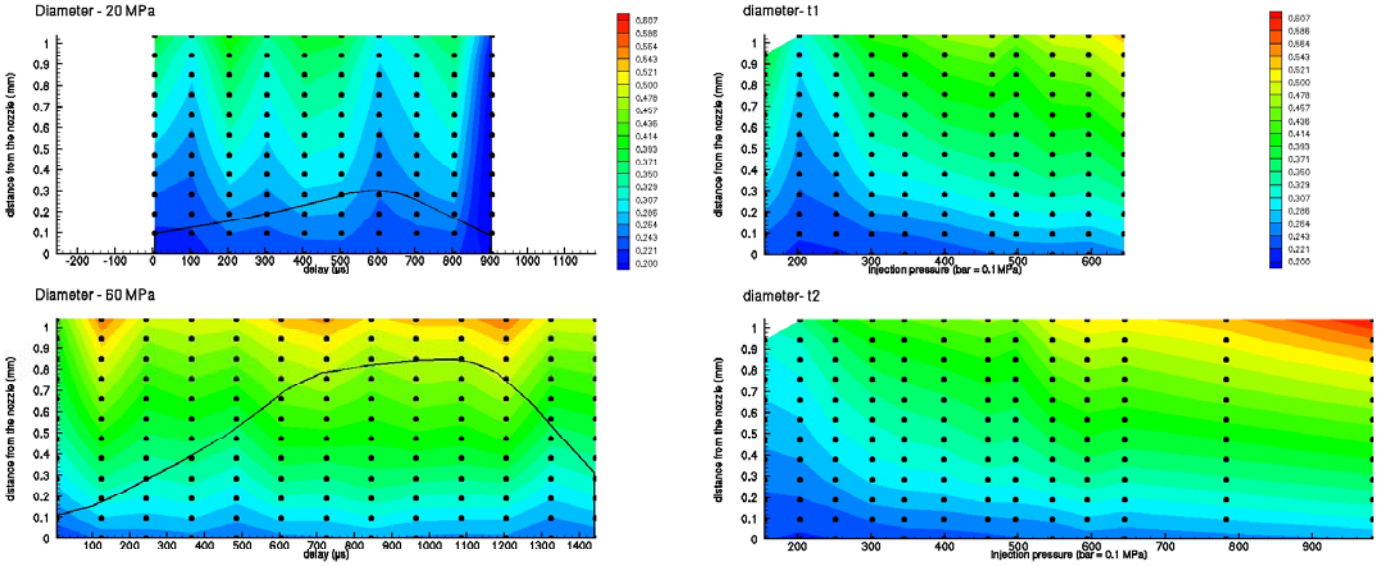

(a) (b)

Fig. 5 Dense core diameter results

The temporal evolution of the dense core diameter ***D*** is presented in Fig. 5(a). Despite the statistical aspect of this study, important fluctuations of this parameter can be observed. For each observed time, the diameter evolution along the jet axis can be considered as linear. But, between two consecutive instants, fluctuations are very significant. For Pi=20 MPa, the mean angle between the jet axis and the interface goes from 4,1° (for t=500 µs) to 2.4° (for t=600µs). For Pi=60 MPa, the interface angle is much greater (7.5° at the delay time t=965µs) and the temporal fluctuations are weaker.
It is difficult to correlate the jet diameter with the temporal evolution of the flow, mostly for the case Pi=20 MPa. Indeed, at this low injection pressure the needle is not fully lifted. This

is due to the lift pressure assistance and can be responsible for a needle lift fluctuation that could perturb the flow. The effect of the injection pressures does not show particular fluctuations of the dense core diameter. This indicates two important things: firstly, the fluctuations observed are time dependent and very reproducible due to the statistical approach. The second statement is that our method used to follow the injection pressure increases for a given type of flow (based on the needle lift) seems to be well adapted. Indeed, during the pressure increase, we stay in the same state of diameter fluctuation. These statements lead us to think that the jet diameter fluctuations are linked to reproducible needle vibrations. These fluctuations could be explained by radial oscillations caused by the surrounding flow that enters the orifice. These radial fluctuations are not detectable on the needle lift curves. The pressure effect (Fig. 5 (b)) shows a progressive increase of the cone angle. Only the results associated to Pi=15 MPa seem to break the curve. At this weak injection pressure, the injection duration is very short and the needle lift is weak. The instant t1 corresponds to the very beginning of the injection and at this time, the observed part of the jet is still protected by the liquid bulk that acts as an aerodynamic shield. The stripping of the jet is then considerably lower than later in the injection and this provokes a deceleration of the injected fluid. This could explain the widening of the jet for this precise operating condition.

The evolution of the jet diameter growth rate δ' with the pressure is represented in Fig. 6. Each dot corresponds to the slope of the linear curve representing the diameter versus the distance from the nozzle. This was computed for each injection pressure and for the two delay times t1 and t2. The vertical tolerance for each point is directly proportional the linear regression coefficient. The point of the series t1 that precedes Pi=55 MPa is distant from the global evolution, but it seems that this slope was extracted from a linear fitting of a curve that was not really linear. The growth rate of the mixing width predicted by a turbulent mixing layer model [7] is also represented in Fig. 6. The experimental points follow this theoretical curve. Indeed, in our experimental conditions, the Reynolds and the Weber number are huge. This implies that the jet is fully turbulent and the surface tension effect is negligible compared to the aerodynamic stress effects on the atomization processes. Thus, the model used by Aupoix[7], based on the Brown and Roshko works [8] can be adapted here to the diameter growth rate δ', with a constant low velocity gas and a liquid speed deduced from the injection pressure thanks to the Bernoulli equation : $\delta' = 0.8\frac{(1-r)(1+\sqrt{s})}{2(1+r\sqrt{s})}$ with s equal to the gas/liquid density ratio and r equal to the gas/liquid velocity ratio. The good fitting of the mixing layer theory shows that large liquid parcels gradually emanate from the jet due to the aerodynamic and turbulence effects. Therefore what we call the "dense core diameter" from the optical approach, corresponds to a liquid phase surrounded by a very dense mixing layer consisting of fuel parcels. The superimposition of

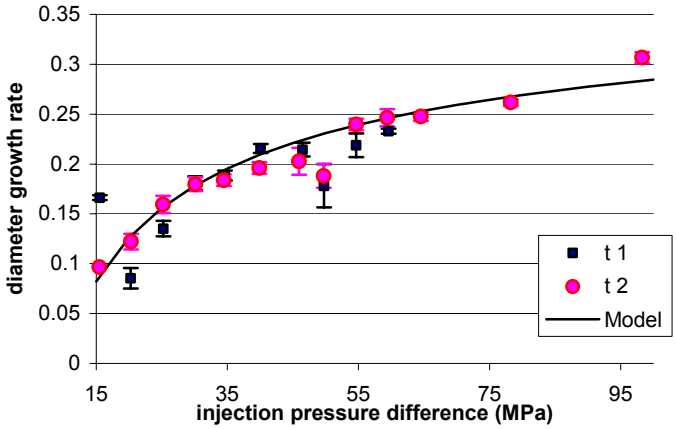

Fig. 6 The effect of the injection pressure on the diameter growth rate.

the images of the fuel parcels on the 2D CCD plane increases the very dense aspect of the mixing layer volume.

5.2. The concavity parameter

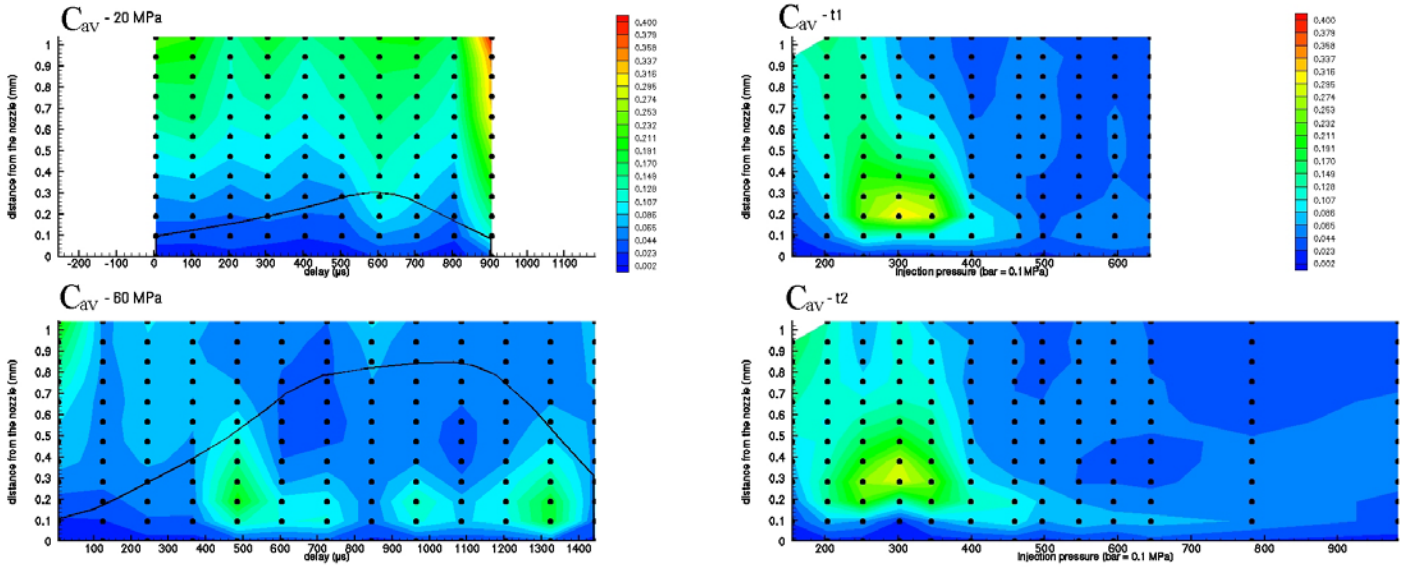

(a) (b)

Fig. 7 Concavity parameter

Fig. 7 presents the results corresponding to the concavity parameter $\boldsymbol{C_{av}}$. The concavity parameter represents the macroscopic disturbances which are not covered by ligaments or liquid parcels. The fluctuations of this parameter for Pi=20 MPa are not directly due to the mean concavity surface fluctuations but probably to the mean jet surface area fluctuations previously observed, and used for the normalization. We observe that the concavity decreases for higher needle lift position. For Pi=60 MPa, the concavity parameter is greater when the flow is accelerating. In fact, we observed on the pictures that this parameter reveals an anomaly of the nozzle. When high values of this parameter are observed, a part of the jet is directly stripped at the nozzle exit, so large ligaments still linked to the jet remain in the binary image and the processing considers this part of the fluid as not yet atomized. These ligaments lead to the appearance of a large area of air laterally embedded between the ligaments and the jet (blue surface in the Fig. 8), that explains the high value of the parameter. This stripping of the jet is repetitively localized on the jet and can correspond to a micro defect at the nozzle exit.

Fig. 8 Concavity surface: P_i=30 MPa, delay time t2=1040 µs

This particular behavior has been observed for the injection pressures close to Pi=30 Mpa (Fig. 7 (b)). In a previous study on the same injector, it was found that this injection range would correspond to the appearance of internal cylindrical gaseous structures linked to the cavitation phenomena [4]. Thus, the jet stripping could be linked to the appearance of cavitation. On the right picture of Fig. 8, we can notice the strong axial asymmetry of the jet morphology. This indicates that the stripping of the jet considerably perturbs the jet atomization. For Pi higher than 30 MPa, this phenomenon disappears. The higher the jet

velocity, the shorter the stripped ligaments. Then, the blue surface in Fig. 8 becomes negligible relative to the jet surface.

5.3. Ligament thickness

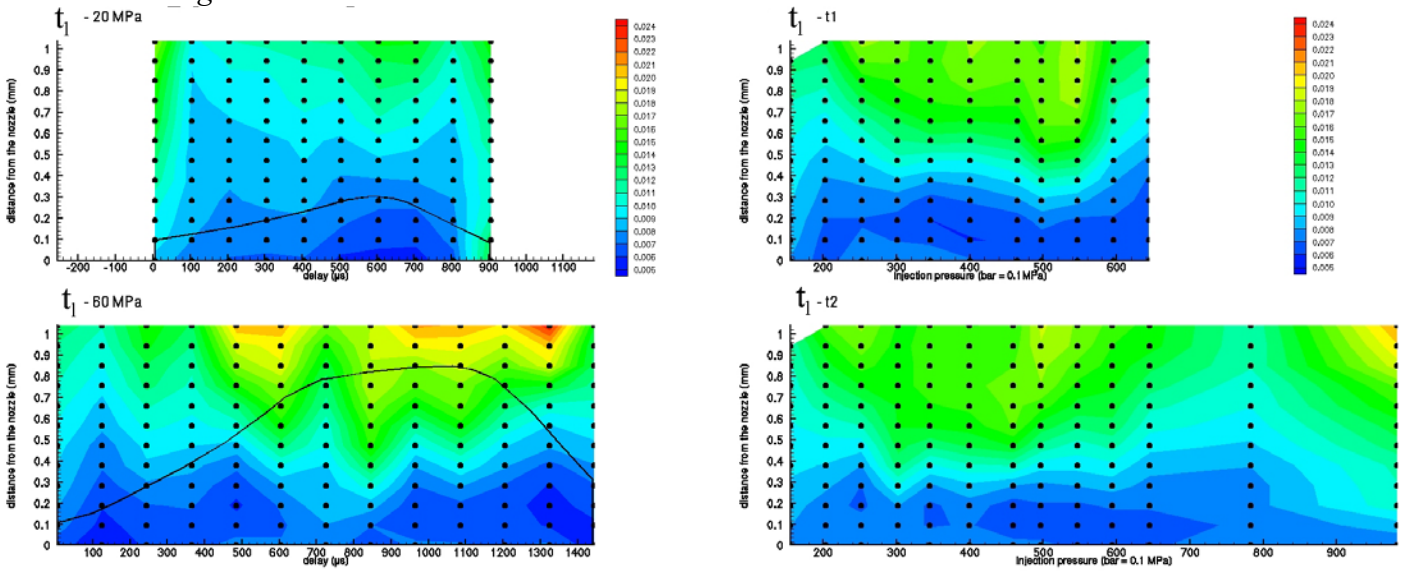

(a) (b)

Fig. 9 Mean ligament thickness

Three parameters characterize the liquid parcels or ligaments that are linked to the dense jet. The first one is t_l, the mean thickness of these structures. The smaller values are found at the beginning of the injection or for low injection pressures, corresponding to the thickness of ligaments about 5-15 µm. On the other hand, the higher values, of the order of 20 µm, correspond to the mean thickness of large liquid blobs separating from the jet. This behavior does not seem to be very sensitive to the pressure variation. In the temporal study, for Pi=60 MPa, the appearance of strong liquid parcels with high thickness seems to correspond to injection times just before and after the quasi-static flow, corresponding to the maximum absolute acceleration of the needle lift.

5.4. Ligament length parameter

Fig. 10 shows the length of the ligaments, l_l. This parameter is normalized by the ROI width. Thus, the value given by this parameter is the mean number of ligaments found in the ROI placed end to end. This number of ligaments takes into account the two visible sides of the interface and possibly a superimposition of different ligaments due to the 3D projection on the image. The mean global number of ligaments observed on one side of the jet picture is found to be between 0.1 and 2.5. The temporal variation of this parameter is different between the Pi=20 & 60 MPa.

For Pi=20 MPa, the mean ligament length is lower during the accelerating flow period, contrary to the Pi=60 MPa case. The reason for this change is linked to the nozzle defect previously observed. For Pi=60 MPa, the ligament formation in the vicinity of the injector due to the nozzle defect is not clearly visible. But the interface is strongly affected by this non-symmetric phenomenon. This is clearly shown by the comparison between the two mean pictures in Fig. 11. Indeed, the mean picture in Fig. 11(b) shows a large zone of intermediate gray level on the upper side of the picture, which contains numerous ligaments. The high number of ligaments observed at the quasi-static flow periods must be the consequence of the internal jet behavior which seems to be dependent on the nozzle defect.

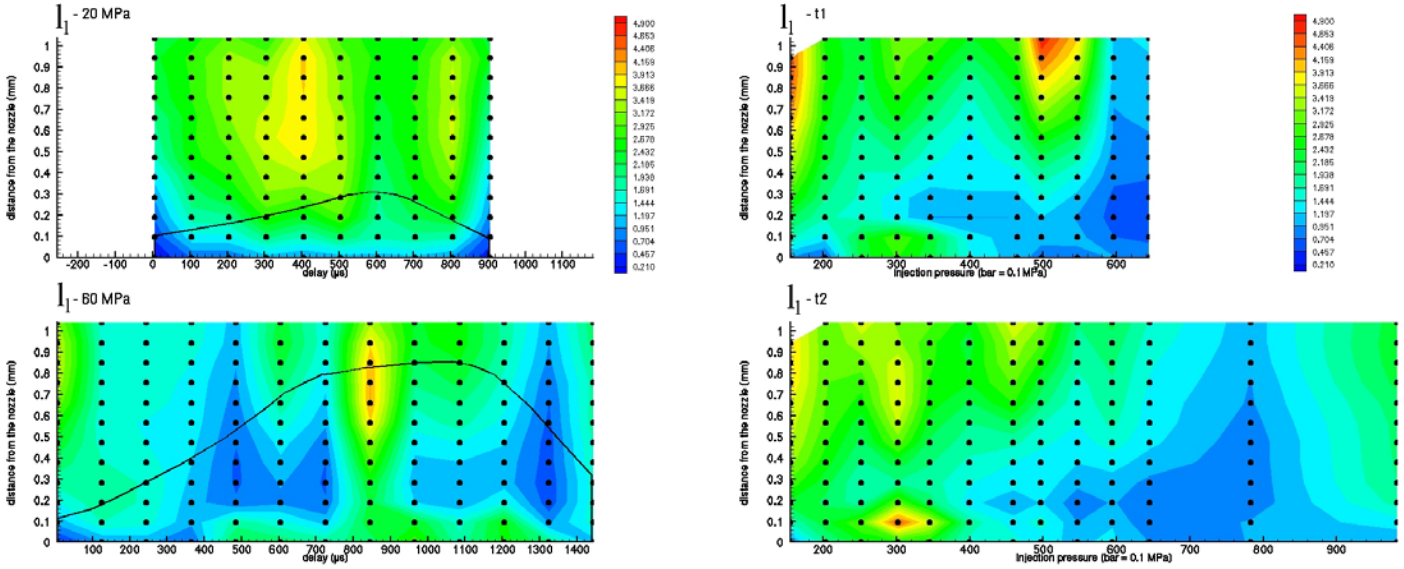

(a) (b)

Fig. 10 mean ligament length

(a) : 20 MPa, delay time = 605 µs (maximum needle lift)

(b) : 60 MPa, delay time = 845 µs (maximum needle lift)

Fig. 11 mean picture of the image processed series

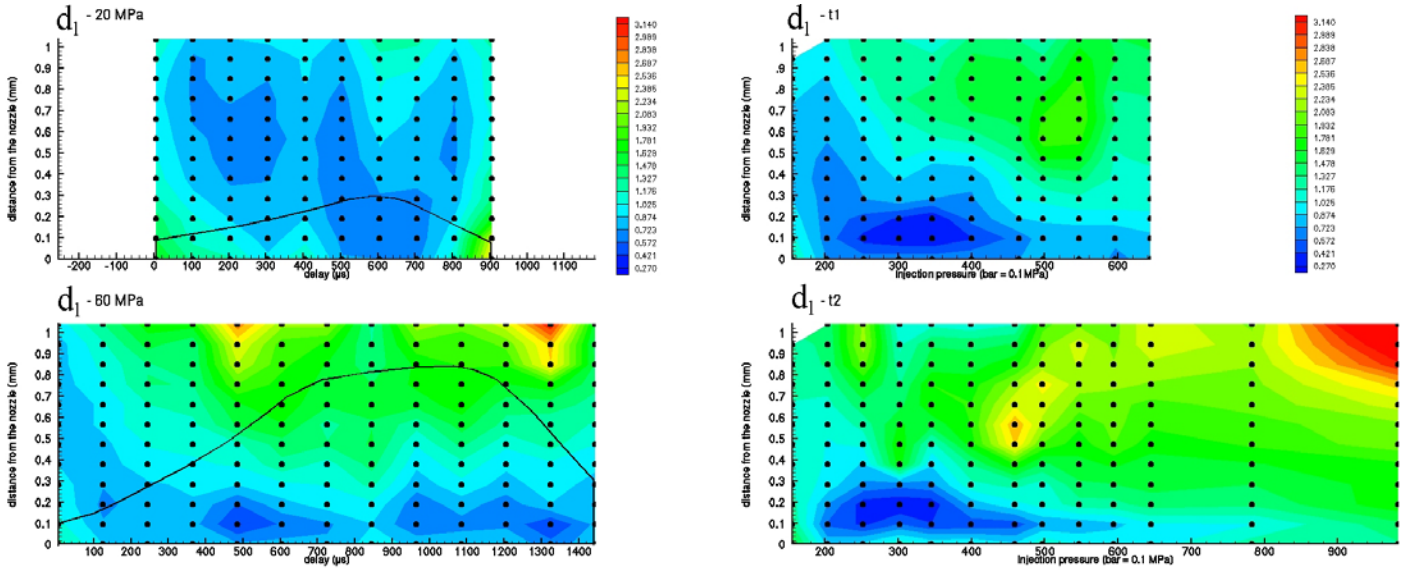

(a) (b)

Fig. 12 mean ligament density

5.5. The ligament density parameter

The ligament density parameter d_l,(Fig. 12) is calculated as the area of the liquid blobs separating from the jet divided by the area of the gaseous zone embedded by these liquid blobs. It can be observed on the temporal analysis that for Pi=20 MPa, the density is globally lower than for Pi=60 MPa due to the lower aerodynamic stresses. For Pi=60 MPa, it is important to note the two high densities observed at the high absolute needle lift acceleration. At these precise times, we previously observed (in Fig. 10) that the length of the liquid blobs was relatively weak. The density parameter informs us that liquid parcels distant from the nozzle are concentrated around the dense core of the jet. Thanks to the pressure evolution, we observe that the higher the injection pressure, the quicker the density increases along the jet axis. In fact, high injection pressure promotes the detachment of liquid parcels that are large and dense compared to the ligament thickness.

6. Conclusion

The statistical morphological analysis permitted quantitative measurements of the Diesel jet interface. The relationship between the morphological parameters and the injection time and pressure shows interesting information.
The visible dense jet diameter D, repetitively fluctuates during the injection for lower injection pressures. The growth of the cone angle with the injection pressure follows the theory of the mixing layer.
A parameter called concavity-parameter C_{av}, enabled us to notice the formation of a ligament at the nozzle outlet, certainly due to a micro manufacturing defect in the orifice or a particular internal flow corresponding to cavitation. This defect seems to strongly perturb the jet atomization with the appearance of abnormal numbers of ligaments.
The ligament thickness l_t, was measured along the jet and shown to be stable with the pressure increase. Further studies are expected to show a possible relationship between the morphological characteristics of the jet at the nozzle outlet and the spray.

7. References

[1] Baev, Bazhaikin, Bichenkov 1980 J. of applied mechanics and technical physics **21** 97-103
[2] Badock, Wirth, Faeth and Leipertz 1999 International Journal of heat and fluid flow **20** 538-54
[3] Faeth, Münch and Leiperts 1997 ICLASS-97 18-22
[4] Yon, Blaisot, Ledoux 2002 ILASS-
[5] Yon, Lalizel, Blaisot 2003 4th Pacific Symposium on Flow Visualization and Image Processing
[6] Yon, Blaisot, 2001 FluVisu-9, Rouen (France).
[7] Aupoix 2002 F282 Forum on turbulent Flows, Montreal
[8] Brown G.L. and Roshko A., 1974 J. Fluid Mech. **64** 775-816